ACS Chemical Neuroscience

Letter

pubs.acs.org/chemneuro

Two-Photon Optical Interrogation of Individual Dendritic Spines with Caged Dopamine

Roberto Araya,[‡,§] Victoria Andino-Pavlovsky,[†] Rafael Yuste,*[,‡] and Roberto Etchenique*[,†]

[†]Departamento de Química Inorgánica, Analítica y Química Física, INQUIMAE, Facultad de Ciencias Exactas y Naturales, Universidad de Buenos Aires, Ciudad Universitaria Pabellón 2 AR1428EHA Buenos Aires, Argentina

[‡]Department of Biological Sciences, Howard Hughes Medical Institute, Columbia University, New York, New York 10027, United States

Supporting Information

ABSTRACT: We introduce a novel caged dopamine compound (RuBi-Dopa) based on ruthenium photochemistry. RuBi-Dopa has a high uncaging efficiency and can be released with visible (blue-green) and IR light in a two-photon regime. We combine two-photon photorelease of RuBi-Dopa with two-photon calcium imaging for an optical imaging and manipulation of dendritic spines in living brain slices, demonstrating that spines can express functional dopamine receptors. This novel compound allows mapping of functional dopamine receptors in living brain tissue with exquisite spatial resolution.

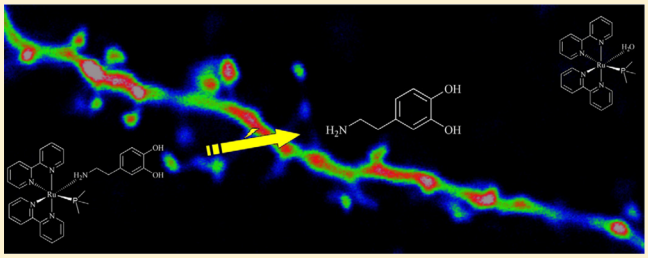

KEYWORDS: *Dopamine, ruthenium, two-photon, caged compound*

Dysfunction of dopaminergic neurotransmission in the CNS underlies a variety of neuropsychiatric disorders, including social phobia,[1] Tourette's syndrome,[2] Parkinson's disease,[3] schizophrenia,[4] neuroleptic malignant syndrome (NMS),[5] attention-deficit hyperactivity disorder (ADHD),[6,7] and drug and alcohol dependence.[8] Dopamine transmission in the brain is mediated by a family of G protein-coupled (GPCR) dopamine receptors named D1 to D5.[3] The D1 receptor[3] has been implicated in motor function,[9,10] cognition,[11,12] and reward.[13,14] However, how dopamine receptors modulate information flow in neuronal circuits, neurons, and synapses is still poorly understood. In fact, there is no unified agreement as to how dopaminergic inputs function and even whether they have an inhibitory or excitatory role on CNS circuits.[15] Understanding these controversies is fundamental to explain why dopaminergic inputs selectively target different brain areas, different neurons, and different postsynaptic sites.

The lack of tools to study dopaminergic inputs with single synaptic resolution has made it difficult to dissect their role at a single neuronal/synapse level and to address fundamental questions on the diversity of dopaminergic inputs and their interaction with excitatory and inhibitory ones. Thus, to study the local function of dopaminergic inputs, it would be ideal to have a highly localized method to activate noninvasively dopamine receptors with a spatial resolution of the size of single synapse.

Local activation of receptors in living neurons can be achieved by two-photon photorelease (uncaging) of caged compounds,[16] since two-photon opto-chemical tools can be used in highly scattering media, such as brain tissue, and afford a spatial resolution of the order of 1 μm.[3] With two-photon uncaging, one can control a given neurotransmitter's physiology and precisely probe the dendritic (or axonal) tree of a neuron, mapping its functional inputs. Indeed, two-photon uncaging of glutamate has revolutionized our current understanding of excitatory transmission and integration in mammalian neurons.[17−20] Using a similar strategy, in this paper, we introduce RuBi-Dopa, the first two-photon caged dopamine compound based on ruthenium-bipyridine chemistry, and use it to optically activate dendritic spines.

The complex $[Ru(bpy)_2(PMe_3)(Dopa)](PF_6)_2$ (bpy = 2,2′ bipyridine, PMe_3 = trimethylphosphine) is a crystalline orange solid synthesized from $[Ru(bpy)_2Cl_2]$ in two steps (see the Supporting Information). It is soluble up to 5 mM in water at pH = 7 and is stable in solution at 37 °C below pH = 8 (although dopamine can be oxidized by air at higher pH). Its ^{1}H NMR spectrum shows the 16 characteristic peaks of bipyridines, corresponding to an asymmetric *cis* complex and the aromatic signals of the coordinated dopamine (Figure S1, see the Supporting Information).

Figure 1 shows the aliphatic portion of its ^{1}H NMR before (top trace) and after 30 s in situ irradiation (bottom trace) with a green LED array (λ = 525 nm, 20 nm fwhm, p = 150 mW). Before irradiation (top trace), the doublet at 0.95, that corresponds to the coordinated trimethylphosphine (PMe_3), is evident. In addition, the triplets A_1 and A_2, at 3.52 and 2.70

Received: March 20, 2013
Accepted: May 14, 2013
Published: May 14, 2013

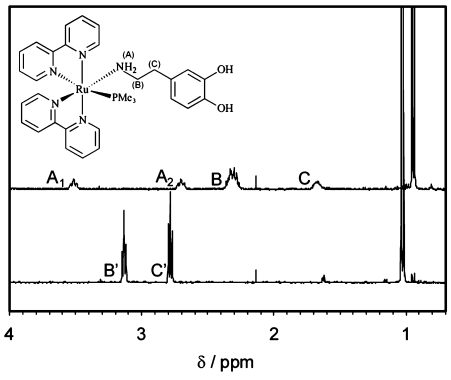

Figure 1. Structure (inset) and aliphatic section of the ^{1}H NMR spectra of RuBi-Dopa in D_2O before (top trace) and after (bottom trace) irradiation into the NMR tube with a 525 nm green LED. The doublets below 1.2 ppm belong to coordinated trimethylphosphine (PMe_3) in RuBi-Dopa (top trace) and in the aquo-complex formed after photoreaction (bottom trace). Signals of coordinated dopamine (B and C) are also apparent. The triplets A_1 and A_2, corresponding to the coordinated $-NH_2$, disappear after irradiation due to rapid exchange with D_2O. The signals of the free dopamine methylenes (B′ and C′) are indicative of the successful photorelease of the ligand.

ppm, respectively, are characteristic of a coordinated amine group. The presence of A_1 and A_2 in D_2O indicates that NH_2 cannot exchange protons, and therefore, the ligand is indeed coordinated through its amine, as is usually the case in Ru-bpy complexes.[21−23]

Furthermore, the adjacent methylenes are strongly shifted to higher fields due to the proximity to Ru^{2+}, and appear as multiplets (Figure 1, signals B and C at 2.30 and 1.78 ppm, respectively). After irradiation the compound successfully photoreleases dopamine. The signals B and C, corresponding to the coordinated ligand, disappear, and the two methylene signals of the free dopamine (B′ and C′) appear at 2.77 and 3.13 ppm respectively. Further addition of dopamine confirmed that the identity of the photoproduct is exclusively this neurotransmitter, and that ligand degradation did not occur throughout the photolysis (data not shown). Moreover, in the aromatic region of the NMR spectra after irradiation, we found the peaks corresponding to the formed aquo-complex $[Ru(bpy)_2(PMe_3)(H_2O)]^{2+}$ and the rest of the dopamine protons (Figure S1, see the Supporting Information), further corroborating the irradiation-induced transition from coordinated-to-free dopamine.

The complex shows the typical metal-to-ligand charge transfer band (^{1}MLCT) found in all the Ru(II)-bipyridyl complexes. Irradiation on this band populates the ^{1}MLCT state, which further decays to a ^{3}MLCT state that can deactivate through emission, or to a dissociative d-d state that promotes the loss of monodentate ligands[24] and the exchange for solvent molecules. In the case of RuBi-Dopa, the only photoproduct detected was dopamine (Figure 1 and Figure S1).

The quantum yield of dopamine photouncaging was measured using UV−vis spectrum analysis of aqueous solutions. Spectra between 350 and 700 nm were obtained during irradiation at right angle with a 405 nm laser diode. The samples were irradiated at open air and not degassed.

The differential amount of products can be calculated with the following expression:

$$\frac{dn_P}{dt} = I_{beam}(1 - 10^{-A_T})\frac{A_R}{A_T}\Phi_{pr} \quad (1)$$

where n_P are the moles of released aquo-complex and dopamine; I_{beam} is the intensity of the laser in Einsteins/s; A_T and A_R are the solution's total absorbance and the reactant's absorbance, respectively; and Φ_{pr} is the photoreaction quantum yield.

Integration of eq 1 was done by a finite differences method. In brief, for an experiment lasting about 1000 s, a measurement every Δt = 2 s was performed. Introducing the values of volume, initial concentration of RuBi-Dopa, molar absorptivities of RuBi-Dopa and its photoproduct and laser power, the amount of photolized complex were calculated for the first interval Δt using eq 1. The new concentration values of RuBi-Dopa and the generated aquo-complex and their respective absorbances were obtained using Beer's law and used to calculate the next intervals. The photorelease quantum yield Φ_{pr} is an adjustable parameter. In this way, not only the initial slope is used to fit Φ_{pr} but the entire set of data, including those in which the absorption of the product is important. Figure 2 (inset) shows a subset of the data during photolysis. The obtained photorelease quantum yield is $\Phi_{pr} = 0.119 \pm 0.011$ ($p < 0.05$) at 37 °C and 0.085 ± 0.004 ($p < 0.05$) at 25 °C.

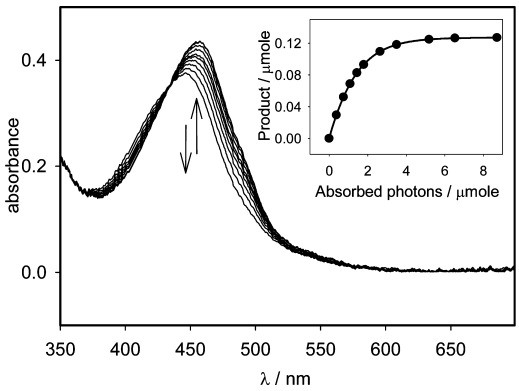

Figure 2. UV−vis spectra of a 75 μM aqueous solution of RuBi-Dopa during photolysis at T = 25 °C and pH = 7. Samples were irradiated at 405 nm, and spectra collected from 350 to 700 nm. Inset: quantum yield calculation using eq 1.

Pinnick and Durham have studied the correlation between the photorelease quantum yield and the MLCT band maximum for several Ru-bpy complexes, finding that both parameters are controlled in a simple way: by the donor ability of the ligands.[24] For an MLCT band centered near 450 nm, a Φ_{pr} around 0.1 is expected, in agreement with our experimental results. Similar values were obtained using 450 and 532 nm irradiation. With its molar absorptivity of about 4900 M^{-1} cm^{-1} at 447 nm, the complex shows very high uncaging sensitivity ($\varepsilon\Phi > 580$) in the visible light region.

Several complexes of this family have been proved to be active in a two-photon regime. Thus, in order to determine the activity of RuBi-Dopa and its two-photon absorption capabilities, we used a solution of RuBi-Dopa, contained in a fluorescence cuvette (1 cm optical path), that was irradiated with an Ti-Sapphire pulsed laser (frequency f = 80 MHz, pulse width τ = 100 fs, λ = 800 nm, average power = 460 mW) and focused on the sample with a 10× objective. With this technique, we found that RuBi-Dopa follows the typical

dx.doi.org/10.1021/cn4000692 | ACS Chem. Neurosci. 2013, 4, 1163−1167

behavior of a two-photon absorption process with emission only at the focal point.

In addition, by using a parametric amplifier (Coherent Legend Elite, f = 1 kHz, τ = 120 fs, λ = 800 nm, average power 730 mW, beam diameter 3 mm fwhm), the instantaneous power of the pulses (6.1×10^9 W) was sufficient to excite RuBi-Dopa without any focusing. Under these conditions, the progress of the photoreaction can be followed from the rather weak fluorescence emission of RuBi-Dopa at ~630 nm (Figure 3). We measured 18 consecutive times the fluorescence

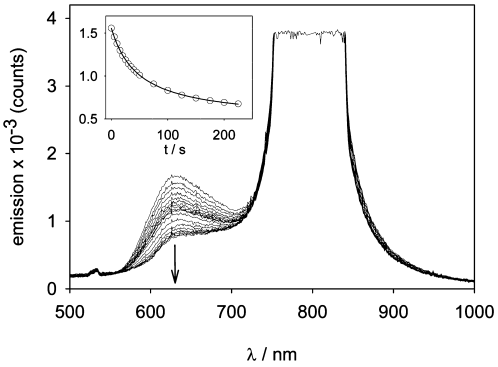

Figure 3. Photolysis of RuBi-Dopa in two-photon regime. A solution containing 22 mM RuBi-Dopa was irradiated with an amplified Ti-Sa laser at 800 nm and the photoreaction followed through its emission band. Inset: time dependence of the emission during photolysis. Details are given in the text.

emission band of RuBi-Dopa (Figure 3), and the peak emission at 630 nm used to calculate the time dependence during photolysis (Figure 3, inset). Being the excitation of RuBi-Dopa at 800 nm, the emission at much higher energies is indicative that a nonlinear process is involved. In addition, by varying the laser power with a reflective filter, to values between 730 and 360 mW, the photolysis rate showed a dependence with the square of the average power, typical of a two-photon excitation regime (Figure S2, Supporting Information). On the other hand, irradiation in the same conditions using a 810 nm, 1.1W LED (Shenzhen Hanhua Opto Co, HH-1WP2IR12-T) did not show any photolysis, ruling out the possibility of detectable linear excitation at this wavelength.

By comparing of the photolysis $t_{1/2}$ of a solution of RuBi-Dopa with a solution of the analogue complex RuBi-Glutamate, which is known to present a functional cross section of 0.14 GM at 800 nm,[23] the same parameter for RuBi-Dopa can be calculated. If the complex concentration, laser power, and irradiation volume are kept constant, then the following expression holds:

$$\sigma_2^{\mathrm{dopa}}\phi_{\mathrm{dopa}} = \sigma_2^{\mathrm{glut}}\phi_{\mathrm{glut}}\frac{t_{1/2}^{\mathrm{glut}}}{t_{1/2}^{\mathrm{dopa}}} = 0.24 \pm 0.04\ \mathrm{GM} \quad (2)$$

With the quantum yield of photorelease of RuBi-glutamate being somewhat higher than that of RuBi-Dopa,[23] this result suggests that the higher functional cross section is due to a higher two-photon absorption.

Once determined that RuBi-Dopa is active in two-photon regime, it can be used to perform an optical manipulation of a 3-D neuronal tissue. Using acute coronal slices of mouse prefrontal cortex, whole-cell patch-clamp recordings from layer five pyramidal cell somata were performed. Dendritic spines (less than 1 μm head diameter) from basal dendrites were selected and placed near or at the center of the microscope field. Since the activation of D1 receptors can trigger intracellular Ca^{2+} signals in cortical neurons,[25] two-photon imaging of spine Ca^{2+} dynamics were performed, after injecting into the cell 200 μM of the calcium indicator Fluo-4 in combination with 200 μM of Alexa-488 to reveal the spine structure (Figure 4A).

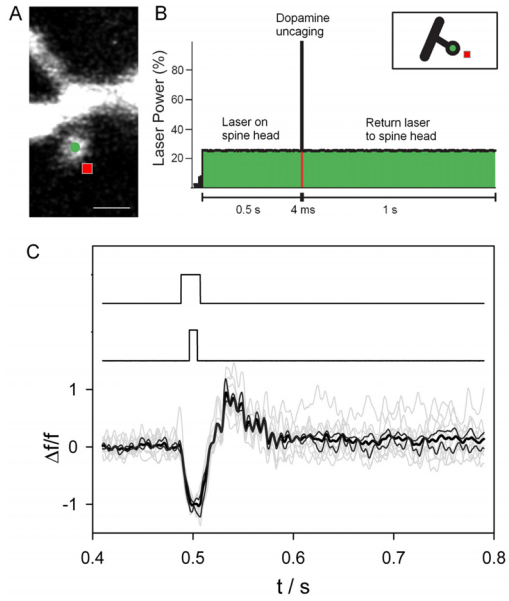

Figure 4. RuBi-Dopa uncaging onto dendritic spines. (A) RuBi-Dopa is bath applied to a cortical slice, and a layer five pyramidal neuron is loaded with 200 μM Fluo-4 Ca^{2+} indicator and 200 μM Alexa-488. Scale bar = 1 μm. (B) Experimental configuration: a Ti-Sapphire laser (820 nm) scans the spine head (at approximately 5−8 mW laser power on sample) first to monitor basal Ca^{2+} concentrations at the location marked with a circle in (A) and then moves to a nearby location (square), where the laser power is increased (to approximately 25 mW on the sample) to uncage dopamine from RuBi-Dopa for 4 ms. After uncaging the laser goes back to initial power and location on the spine head. (C) Spine fluorescent signals (bottom traces; individual traces in gray (n = 10), average trace in bold black, and ± StEr traces in black) showing a sudden increase of Ca^{2+} concentration after the two-photon uncaging of dopamine. The middle trace shows the uncaging pulse. The fluorescent signal detection, by a photomultiplier tube (PMT), was blocked for a few milliseconds before, during, and after the uncaging pulse with the use of an ultrafast shutter (top trace) to prevent potential PMT saturation and errors in signal detection.

A 300 μM RuBi-Dopa solution was applied to the bath, and a Ti-Sapphire pulsed laser (Coherent Chameleon Ultra II, f = 80 MHz, τ = 140 fs) with a high numerical aperture objective (60×, 0.9NA, water immersion objective) was used at 725 nm to image the spine and uncover its morphological features. The wavelength was switched to 820 nm to uncage RuBi-Dopa right next to the spine head (red dot in Figure 4) and monitor spine head Ca^{2+} accumulations before and after RuBi-Dopa uncaging (Figure 4, green dot).

Uncaging experiments were performed in neurons clamped at a resting potential of −65 mV, and bathed at 37 °C. The amount of current needed to hold the layer five pyramidal neurons at this resting potential did not differ before and after bath application of RuBi-Dopa (data not shown). These results

dx.doi.org/10.1021/cn4000692 | ACS Chem. Neurosci. 2013, 4, 1163−1167

suggest that the cell is not affected by the presence of RuBi-Dopa in the bath. A 4 ms two-photon irradiation pulse right next to the spine head elicited the release of dopamine from the RuBi-Dopa complex and a rapid increase in spine Ca^{2+} concentration in 11 of 13 spines tested (for one responsive spine, see example in Figure 4), indicating both the successful photorelease of dopamine and the presence of functional dopamine receptors on the spine, as suggested by previous studies of D1 receptor immunoreactivity.[26−29] Indeed, addition of the specific D1 receptor blocker[30] SCH 23390, at a concentration previously shown to be specific for D1 receptors in these neurons,[31] completely blocked the evoked spine Ca^{2+} signals recorded after uncaging of RuBi-Dopa (Figure S3, see the Supporting Information). Interestingly, in only 2 of the 13 spines tested, no Ca^{2+} signals were observed at the spine head after the two-photon uncaging of dopamine, suggesting that some spines in layer five pyramidal neurons may not have functional dopamine receptors. Simultaneous current clamp measurements demonstrated that the Ca^{2+} release in the spine does not induce important voltage changes into the cell soma (see the Supporting Information for details), and therefore, the dopaminergic activation of spines would go unnoticed with electrophysiological techniques.

These results demonstrate the capability of RuBi-Dopa as a tool for activating single spines, which arises from its two-photon sensitivity, a characteristic that just a few caged compounds have. We have performed an optical activation and functional optical measurement of various spines after two-photon uncaging of RuBi-Dopa. Our experiments required the injection of the Ca^{2+} indicator via the recording patch electrode. Thus, in order to perform a full-optical functional mapping of dopaminergic transmission at a single spine level, one could combine the use of RuBi-Dopa uncaging and a neuronal-specific genetically encoded calcium indicator (e.g., GCaMP). By using these techniques, it is possible to bypass the invasive characteristics of standard electrophysiological techniques.

At the concentration of RuBi-Dopa used in this study, we did not observe any morphological or functional deleterious effect in the spine functional and morphological characteristics (marked by the reliability of the calcium responses) nor any damage of the spine head after two-photon uncaging of RuBi-Dopa. The lack of acute phototoxicity at the cellular and single spine level could be due to the fact that no radicals are generated in the photoreaction of RuBi-Dopa, since the Ru−N bond is cleaved heterolytically, yielding two entire molecules. However, we cannot completely rule out a potential toxicity effect in experiments at longer time courses.

In conclusion, we have developed a caged dopamine (RuBi-Dopa), a novel tool for opto-manipulation and investigation of dopaminergic transmission of a subcellular neuronal entity, a single dendritic spine, with high spatial and temporal resolution by means of two-photon uncaging. Chemically, to our knowledge, this is the first design of a two-photon active caged dopamine. Biologically, this is the first proof of principle that dopamine can be released with two-photon precision in single dendritic spines, the main receptacles of excitatory information in the brain, and generate a local Ca^{2+} response. This novel compound together with state-of-the-art techniques such as two-photon excitation and calcium imaging allows the mapping of functional dopamine receptors in brain tissue with exquisite spatial resolution in a noninvasive way.

■ ASSOCIATED CONTENT

Supporting Information

Synthesis of the complex, ^1H NMR spectra during photolysis, and additional neurophysiological data. This material is available free of charge via the Internet at http://pubs.acs.org.

■ AUTHOR INFORMATION

Present Address

[§]R.A.: Département de Physiologie, Université de Montréal, 2960 Chemin de la Tour, Montréal, Québec H3T 1J4, Canada.

Author Contributions

R.A., V.A., R.Y. and R.E. conceived and designed the experiments. R.A., V.A. and R.E. performed the experiments. R.A. and R.E. analyzed the data. R.A., R.Y. and R.E. wrote the manuscript.

Funding

V.A. and R.E. were supported by CONICET, UBA and ANPCyT. R.A. and R.Y. were supported by the Kavli Institute for Brain Science, NEI, NINDS, NIHM, NIDA, MURI program, Keck Foundation and NARSAD.

Notes

R.E. is staff of CONICET.

The authors declare no competing financial interest.

■ REFERENCES

(1) Schneier, F. R., Liebowitz, M. R., Abi-Dargham, A., Zea-Ponce, Y., Lin, S. H., and Laruelle, M. (2000) Low dopamine D(2) receptor binding potential in social phobia. *Am. J. Psychiatry 157*, 457.

(2) Mink, J. W. (2006) Neurobiology of basal ganglia and Tourette syndrome: basal ganglia circuits and thalamocortical outputs. *Adv. Neurol. 99*, 89−98.

(3) Beaulieu, J. M., and Gainetdinov, R. R. (2011) The physiology, signaling, and pharmacology of dopamine receptors. *Pharmacol. Rev 63*, 182−217.

(4) Eyles, D., Feldon, J., and Meyer, U. (2012) Schizophrenia: do all roads lead to dopamine or is this where they start? Evidence from two epidemiologically informed developmental rodent models. *Transl. Psychiatry 2*, e81.

(5) Adnet, P., Lestavel, P., and Krivosic-Horber, R. (2000) Neuroleptic malignant syndrome. *Br. J. Anaesthesia 85*, 129−135.

(6) Swanson, J. M., Kinsbourne, M., Nigg, J., Lanphear, B., Stefanatos, G. A., Volkow, N., Taylor, E., Casey, B. J., Castellanos, F. X., and Wadhwa, P. D. (2007) Etiologic subtypes of attention-deficit/hyperactivity disorder: brain imaging, molecular genetic and environmental factors and the dopamine hypothesis. *Neuropsychol. Rev. 17*, 39−59.

(7) Gizer, I. R., Ficks, C., and Waldman, I. D. (2009) Candidate gene studies of ADHD: a meta-analytic review. *Hum. Genet. 126*, 51−90.

(8) Kienast, T., and Heinz, A. (2006) Dopamine and the diseased brain. *CNS Neurol. Disord.: Drug Targets 5*, 109−131.

(9) Gerfen, C. R. (2000) Molecular effects of dopamine on striatal-projection pathways. *Trends Neurosci. 23*, S64−70.

(10) Campanella, G., Roy, M., and Barbeau, A. (1987) Drugs affecting movement disorders. *Annu. Rev. Pharmacol. Toxicol. 27*, 113−136.

(11) Williams, G. V., and Goldman-Rakic, P. S. (1995) Modulation of memory fields by dopamine D1 receptors in prefrontal cortex. *Nature 376*, 572−575.

(12) Zahrt, J., Taylor, J. R., Mathew, R. G., and Arnsten, A. F. (1997) Supranormal stimulation of D1 dopamine receptors in the rodent prefrontal cortex impairs spatial working memory performance. *J. Neurosci. 17*, 8528−8535.

(13) Self, D. W., Barnhart, W. J., Lehman, D. A., and Nestler, E. J. (1996) Opposite modulation of cocaine-seeking behavior by D1- and D2-like dopamine receptor agonists. *Science 271*, 1586−1589.

(14) Smith-Roe, S. L., and Kelley, A. E. (2000) Coincident activation of NMDA and dopamine D1 receptors within the nucleus accumbens core is required for appetitive instrumental learning. *J. Neurosci. 20*, 7737−7742.
(15) Girault, J. A., and Greengard, P. (2004) The neurobiology of dopamine signaling. *Arch. Neurol. 61*, 641−644.
(16) Denk, W., Strickler, J. H., and Webb, W. W. (1990) Two-photon laser scanning fluorescence microscopy. *Science 248*, 73−76.
(17) Araya, R., Eisenthal, K. B., and Yuste, R. (2006) Dendritic spines linearize the summation of excitatory potentials. *Proc. Natl. Acad. Sci. U.S.A. 103*, 18799−18804.
(18) Araya, R., Jiang, J., Eisenthal, K. B., and Yuste, R. (2006) The spine neck filters membrane potentials. *Proc. Natl. Acad. Sci. U.S.A. 103*, 17961−17966.
(19) Matsuzaki, M., Ellis-Davies, G. C. R., Nemoto, T., Miyashita, Y., Iino, M., and Kasai, H. (2001) Dendritic spine geometry is critical for AMPA receptor expression in hippocampal CA1 pyramidal neurons. *Nat. Neurosci. 4*, 1086−1092.
(20) Matsuzaki, M., Honkura, N., Ellis-Davies, G. C. R., and Kasai, H. (2004) Structural basis of long-term potentiation in single dendritic spines. *Nature 429*, 761−766.
(21) Zayat, L., Salierno, M., and Etchenique, R. (2006) Ruthenium-(II) bipyridyl complexes as photolabile caging groups for amines. *Inorg. Chem. 45*, 1728−1731.
(22) Zayat, L., Noval, M. G., Campi, J., Calero, C. I., Calvo, D. J., and Etchenique, R. (2007) A new inorganic photolabile protecting group for highly efficient visible light GABA uncaging. *ChemBioChem 8*, 2035−2038.
(23) Salierno, M., Marceca, E., Peterka, D. S., Yuste, R., and Etchenique, R. (2010) A fast ruthenium polypyridine cage complex photoreleases glutamate with visible or IR light in one and two photon regimes. *J. Inorg. Biochem. 104*, 418−422.
(24) Pinnick, D. V., and Durham, B. (1984) Photosubstitution Reactions of $Ru(bpy)_2XY^{n+}$ Complexes. *Inorg. Chem. 23*, 1440−1445.
(25) Lezcano, N., and Bergson, C. (2002) D1/D5 dopamine receptors stimulate intracellular calcium release in primary cultures of neocortical and hippocampal neurons. *J. Neurophysiol. 87*, 2167−2175.
(26) Smiley, J. F., Levey, A. I., Ciliax, B. J., and Goldman-Rakic, P. S. (1994) D1 dopamine receptor immunoreactivity in human and monkey cerebral cortex: predominant and extrasynaptic localization in dendritic spines. *Proc. Natl. Acad. Sci. U.S.A. 91*, 5720−5724.
(27) Bergson, C., Mrzljak, L., Smiley, J. F., Pappy, M., Levenson, R., and Goldman-Rakic, P. S. (1995) Regional, cellular, and subcellular variations in the distribution of D1 and D5 dopamine receptors in primate brain. *J. Neurosci. 15*, 7821−7836.
(28) Yung, K. K., Bolam, J. P., Smith, A. D., Hersch, S. M., Ciliax, B. J., and Levey, A. I. (1995) Immunocytochemical localization of D1 and D2 dopamine receptors in the basal ganglia of the rat: light and electron microscopy. *Neuroscience 65*, 709−730.
(29) Bordelon-Glausier, J. R., Khan, Z. U., and Muly, E. C. (2008) Quantification of D1 and D5 dopamine receptor localization in layers I, III, and V of Macaca mulatta prefrontal cortical area 9: coexpression in dendritic spines and axon terminals. *J. Comp. Neurol. 508*, 893−905.
(30) Bourne, J. A. (2001) SCH 23390: The first selective dopamine D-1-like receptor antagonist. *CNS Drug Rev. 7*, 399−414.
(31) Rotaru, D. C., Lewis, D. A., and Gonzalez-Burgos, G. (2007) Dopamine D1 receptor activation regulates sodium channel-dependent EPSP amplification in rat prefrontal cortex pyramidal neurons. *J. Physiol. 581*, 981−1000.